# A Novel Method for the Extraction, Purification, and Characterization of Noble Gases in Produced Fluids

R. L. Tyne, P. H. Barry, D. J. Hillegonds, A. G. Hunt, J. T. Kulongoski, M. J. Stephens, D. J. Byrne, C. J. Ballentine

# Geochemistry, Geophysics, Geosystems

# A Novel Method for the Extraction, Purification, and Characterization of Noble Gases in Produced Fluids

R. L. Tyne[1] (iD), P. H. Barry[2] (iD), D. J. Hillegonds[1], A. G . Hunt[3], J. T. Kulongoski[4] (iD), M. J. Stephens[5] (iD), D. J. Byrne[6], and C. J. Ballentine[1] (iD)

[1]Department of Earth Sciences, University of Oxford, Oxford, UK, [2]Department of Marine Chemistry and Geochemistry, Woods Hole Oceanographic Institution, Woods Hole, MA, USA, [3]Denver Federal Center, USGS, Denver, CO, USA, [4]California Water Science Center, USGS, San Diego, CA, USA, [5]California Water Science Center, USGS, Sacramento, CA, USA, [6]CRPG-CNRS, Université de Lorraine, Nancy, France

**Abstract** Hydrocarbon systems with declining or viscous oil production are often stimulated using enhanced oil recovery (EOR) techniques, such as the injection of water, steam, and $CO_2$, in order to increase oil and gas production. As EOR and other methods of enhancing production such as hydraulic fracturing have become more prevalent, environmental concerns about the impact of both new and historical hydrocarbon production on overlying shallow aquifers have increased. Noble gas isotopes are powerful tracers of subsurface fluid provenance and can be used to understand the impact of EOR on hydrocarbon systems and potentially overlying aquifers. In oil systems, produced fluids can consist of a mixture of oil, water and gas. Noble gases are typically measured in the gas phase; however, it is not always possible to collect gases and therefore produced fluids (which are water, oil, and gas mixtures) must be analyzed. We outline a new technique to separate and analyze noble gases in multiphase hydrocarbon-associated fluid samples. An offline double capillary method has been developed to quantitatively isolate noble gases into a transfer vessel, while effectively removing all water, oil, and less volatile hydrocarbons. The gases are then cleaned and analyzed using standard techniques. Air-saturated water reference materials ($n = 24$) were analyzed and results show a method reproducibility of 2.9% for $^4$He, 3.8% for $^{20}$Ne, 4.5% for $^{36}$Ar, 5 .3% for $^{84}$Kr, and 5.7% for $^{132}$Xe. This new technique was used to measure the noble gas isotopic compositions in six produced fluid samples from the Fruitvale Oil Field, Bakersfield, California.

## 1. Introduction

The increasing use of enhanced oil recovery (EOR) and other techniques to increase hydrocarbon recovery such as hydraulic fracturing has led to concerns that shallow aquifers could be contaminated due to these more intensive hydrocarbon production practices (Darrah et al., 2014, 2015; Gilfillan et al., 2017; Harkness et al., 2017; Vengosh et al., 2014). It is imperative to understand subsurface fluid provenance and dynamics when investigating such systems. In systems with long hydrocarbon production histories, it is valuable to determine the pristine signature (before EOR) and how the system has evolved geochemically with production; injected fluids play a significant role on this evolution. Noble gases represent powerful geochemical tracers, as they are chemically inert and therefore act conservatively in geologically dynamic systems (e.g., Ballentine et al., 1991, 1996, 2002; Barry, Kulongoski, et al., 2018; Barry, Lawson, et al., 2018; Bosch & Mazor, 1988; Darrah et al., 2015; Gilfillan et al., 2008, 2014; Holland & Gilfillan, 2013; Pinti & Marty, 1995). Noble gases are most readily determined in systems dominated by a single phase (e.g., gas or groundwater); however, within a hydrocarbon system they can reside in multiple phases (i.e., oil, water and gas) and thus may be present in each component.

Terrestrial reservoirs of noble gases (atmospheric, crustal, and mantle) have well-characterized and diagnostic isotopic and abundance compositions, meaning fluid contributions from each reservoir can be easily differentiated. Previous studies have successfully used noble gas isotopes and abundances to quantify water-oil-gas interactions in both conventional and unconventional hydrocarbon systems and those effected by EOR techniques (Ballentine et al., 1991, 1996, 2002; Barry et al., 2016, 2017; Barry, Kulongoski, et al., 2018; Barry, Lawson, et al., 2018; Byrne et al., 2018a, 2018b; Darrah et al., 2014, 2015; Györe et al., 2017, 2015; Prinzhofer, 2013). These studies have primarily focused on natural gas systems, although some have specifically investigated oil systems (e.g., Ballentine et al., 1996; Györe et al., 2017), unconventional systems (e.g.,

Byrne et al., 2018b; Zhou et al., 2005) and multi-component systems (Barry, Lawson, et al., 2018). The use of noble gases as tracers in oil-dominated systems is not yet well established due to the multiphase nature of these samples meaning they are not amenable to the normal high-vacuum noble gas purification procedures for natural gases. As a result, the focus of previous studies has been primarily on gas phase hydrocarbon samples, which are exsolved from oil as they decompress during production (Figure S1 in the supporting information; Ballentine et al., 2002; Prinzhofer, 2013). Recent studies reconstructed the noble gas composition of the oil phase from casing gas measurements using broad assumptions about gas solubility in oil (e.g., Barry, Kulongoski, et al., 2018; Barry, Lawson, et al., 2018). However, production practices are often not amenable to collecting casing gas samples, and therefore produced fluids must be used to geochemically characterize the hydrocarbon reservoir. Additionally, if casing gas flow is controlled or diverted during production, produced waters samples may provide a better representation of reservoir conditions.

We present a new method for isolating noble gases from produced fluids, containing water-gas-oil mixtures. The technique required construction of an offline extraction system, which interfaced with existing purification systems and two noble gas mass spectrometers (Thermo Argus VI and Thermo Helix SFT). New composition and isotope data for air-saturated waters (ASW) are reported. The precision, accuracy and reproducibility of both ASW and produced fluid samples measured are assessed using the new method. Produced fluid data indicate that this technique is robust at isolating and measuring noble gas isotope compositions in oil-water-gas mixtures and can be used to investigate processes within hydrocarbon reservoirs.

## 2. Analytical Methods

Noble gas analyses were conducted in the Noble Laboratory at the University of Oxford, UK, where the analysis of gas phase samples is well established using a custom-built high vacuum gas purification system to purify and separate noble gas species before measurement (e.g., Barry et al., 2016, 2017; Barry, Kulongoski, et al., 2018; Barry, Lawson, et al., 2018; Byrne et al., 2018a, 2018b). Samples containing significant liquid volumes cannot be analyzed in this way, as the liquids are not adequately removed using conventional cryogenic or gettering techniques, are adsorbed easily to the inside of the stainless-steel system and are difficult to remove even using ultra-high vacuum turbomolecular and diaphragm pump combinations. Single-phase water samples are routinely characterized in other laboratories (e.g., Bayerle et al., 2000; Hunt, 2015). However, the introduction of hydrocarbons into these types of systems will contaminate the mass-spectrometers and increase backgrounds and isobaric interferences, significantly reducing measurement precision and reliability. A new inlet line and vacuum system were developed for the extraction of the noble gases from multi-phase fluid samples using a double capillary method to quantitatively transfer all the noble gases. Water vapor in the system is cryogenically drawn across the capillary towards a stainless-steel cold trap cooled to $-196$ °C. The strong flow of water vapor entrains the noble gases and quantitatively draws them across towards the cold trap, preventing any backflow of noble gases and resulting in their isolation in the transfer vessel (Bayerle et al., 2000). The capillaries were effective at isolating the noble gases in the transfer vessel and minimizing water transfer; the liquid volume transferred was typically less than 0.5 ml compared to the initial sample size of approximately 13 ml. The transfer vessel is later attached to a gas purification system (Figure 1). The extraction line system consists of high-vacuum circular knife-edge (ConFlat fittings) fittings with copper flanges, VCR fittings with silver-coated stainless-steel gaskets and bellow-sealed valves. It is split into two volumes (A and B), and the Cu tube, which interfaces the sample to the extraction system. Volume A represents the dedicated inlet section and is comprised of a degassing volume and a 1-mm (inside diameter, ID) by 30-mm capillary on the horizontal between the degassing vessel and the transfer vessel. The 1mm capillary is included to minimize the transfer of water and low-volatility hydrocarbons out of the transfer vessel. In volume B, the noble gases are stored and transferred to the gas purification system; it includes a 0.5-mm ID by 30-mm capillary screwed into a solid Cu disk below valve E2.

Initially volumes A and B are pumped to low-vacuum (to $<2 \times 10^{-2}$ mbar) using a rotary pump and then to high-vacuum using a turbo molecular pump (to $<3 \times 10^{-6}$ mbar). Valves E2 and E3 are then closed and the bottom of volume B (up where the vessel separates to the two valves) is cooled to $-196$ °C using a liquid nitrogen bath. Volume A is heated to 600 °C using a thermostatically controlled heater, whilst being actively
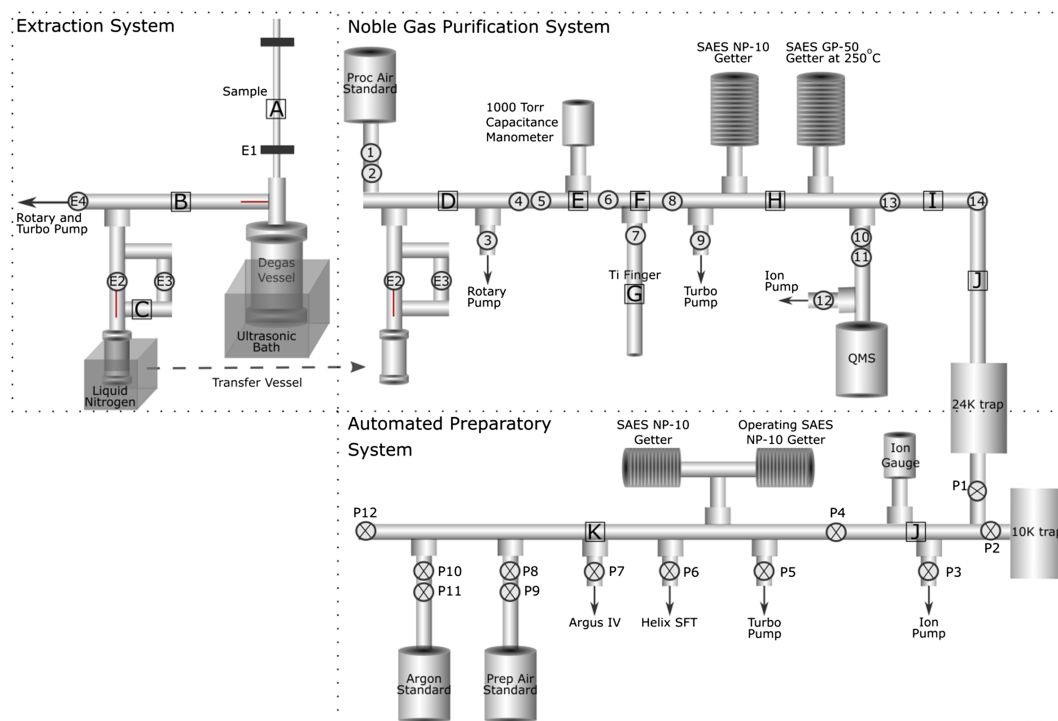
**Figure 1.** Schematic diagram of the noble gas extraction system, noble gas purification system and automated preparatory system. The systems are constructed of stainless steel with high-vacuum circular knife-edge (ConFlat [CF] fittings) fittings with copper flanges and bellow-sealed valves, with the exception of the fittings to both the vessels on the extraction systems, which are ¼" VCR fittings with silver-coated stainless steel gaskets. The procedure is split across three different systems (extraction, noble gas purification and automated preparatory) with 11 distinct volumes held at vacuum by turbomolecular pumps. The Hidden Analytical HAL-200 quadrupole mass spectrometer (QMS) on the gas purification system is held separately at vacuum by a dedication ion pump. The procedural air standard was collected in a cylinder from University Parks, Oxford, UK on 24 November 2014 (pressure: 1027mBar, temperature: 5 °C and humidity: 89%). The prep air standard was collected in a cylinder from University Parks on 13 May 2016 (pressure: 1,010 mBar, temperature: 14 °C, and humidity: 71%).

pumped. After 3 min, E4 is closed and the sample is released into the extraction volume by opening clamp E1, with valves E2-E4 closed. The Cu tube sample and volume A are then heated (using a thermostatically controlled heater at 600 °C) for an additional 3 min. Valve E2 is then opened to allow for the cryogenic transfer of noble gases and water vapor across the capillary into volume B. To further facilitate the degassing of the sample and noble gas transfer, the degassing vessel is agitated in an ultra-sonic bath and the sample tube and capillaries are heated (as above) for 2 min every 15 min, to ensure the system stays at temperature. After 1 hr, valve E2 is closed and the transfer vessel is moved to the dedicated gas purification system. The extraction of noble gases from water typically takes between 18 and 30 min (e.g., Hunt, 2015). In implementing a double capillary method for the produced fluids, the transfer time was increased to 1 hr to establish a safety margin ensuring quantitative gas transfer into the transfer vessel and sufficient water vapor accumulation to enable quantitative gas transfer back out of the transfer vessel onto the noble gas purification system.

Once extracted, the transfer vessel is moved to a gas purification line. The noble gases are transferred back through the capillary by establishing a flow of water vapor from the transfer vessel onto a titanium sponge held at 950 °C. Details about the subsequent purification and analysis steps can be found in the supporting information (Barry et al., 2016, SAES Getters, 1986, Stout & Gibbons, 1955). In addition, the supporting information contains information on the types of standards, blanks and corrections used.

After the gases are extracted, the relative amounts of gas ($V_g$ [cm$^3$]), water ($V_w$ [cm$^3$]), and oil ($V_o$ [cm$^3$]) in each Cu tube are measured using the full Cu tube volume ($V_t$=length*pi*(ID/2)$^2$), the weight of sample processed, and the ratio of oil-water collected within the degas vessel, after the extraction of each sample (Table 1).

**Table 1**
*Oil Metadata for the Produced Waters From the Fruitvale Oil field*

| Sample ID | Production conditions | | API | Volumes sampled | | | GORs | WORs |
|---|---|---|---|---|---|---|---|---|
| | Temperature | Salinity | | Oil | Gas | Water | | |
| | °C | M | o | cm$^3$ | cm$^3$ | cm$^3$ | | |
| F1 | 29 | 0.095 | 18.5 | 0 | 0.5 | 12.9 | 76 | 41 |
| F2 | 36 | 0.095 | 18.5 | 0 | 0.8 | 12.4 | 75 | 17 |
| F3 | 35 | 0.095 | 18.5 | 0.3 | 0.6 | 12.4 | 75 | 147 |
| F4 | 36 | 0.095 | 18.5 | 0 | 0.4 | 12.9 | 75 | 25 |
| F5 | 36 | 0.095 | 18.5 | 0 | 0.4 | 12.9 | 76 | 28 |
| F6 | 43 | 0.095 | 16.7 | 0 | 0.7 | 12.7 | 48 | 39 |

*Note.* Volumes sampled are those in the Cu tube measured in the laboratory. All other information is from the California Division of Oil Gas and Geothermal Resources (DOGGR) (2018). GORs and WORs are the gas-oil ratio and water-oil ratio, respectively, for the production well during the month of sampling. For additional data see Table S2.
Abbreviations: GOR: gas-oil ratio; WOR: water-oil ratio.

As it is highly probable that an oily residue remains within the extraction system, the system (past E4) is dismantled and cleaned after each extraction. Parts are washed and sonicated in an acetone bath to remove any oily residue and then placed in an oven at 100 °C for a minimum of 1 hr to remove the acetone. The parts are then scrubbed with a plastic brush and neutracon detergent (Decon) and rinsed in DI water, to ensure the removal of any leftover salt before being returned to the oven for 1 hr. Parts are also washed with Petroleum Ether and left to dry for 1 hr under a fume hood. The system is then reassembled and He leak checked.

## 3. Air-Saturated Water Data

ASWs were used as a reference material for checking the method reproducibility and calibrating sample measurements. These were chosen over an air standard, as they are more comparable to the samples. Due to the length of time that is required to run an ASW, only 24 have been analyzed.

### 3.1. Air-Saturated Water Generation

ASWs were made in the Oxford Noble Laboratory, by equilibrating 20 L of water in a plastic carboy with the atmosphere. Equilibration is ensured using an aquarium bubbler (bubbling at a rate of 2 L/min) suspended in the water (Hillegonds et al., 2013). Water is bubbled for a minimum of seven days with the laboratory air temperature next to the carboy recorded every 15 min. Temperature variations are typically ±0.2 °C. The bubbler is stopped at least 3 hr prior to sampling of the ASWs. The noble gas concentrations in the ASW generated are as expected under those conditions.

ASW samples were taken in copper tubes held in clamp holders to ensure consistent liquid volume. The final equilibration temperature was taken as the average air temperature of the 48 hr prior to sampling.

ASW were extracted using the method described in this paper and were analyzed between every three unknown samples of the system.

### 3.2. Calculating Air-Saturated Water concentrations

The concentration of each noble gas in ASW can be calculated using Henry's Law solubility equilibrium. The expected concentration (cm$^3$/cm$^3$) in the ASW under laboratory conditions can be calculated using:

$$C_i^{\text{ex asw}} = \frac{\left(760 - e^{\left(-5375.83/T + 21.2023734\right)}\right) \times P_i}{18.02 \times 760 \times K_i^{gw}} \times e^{\left(h/8350\right)} \tag{1}$$

where $C_i^{\text{ex asw}}$ is the expected concentration of $i$ in the ASW, $h$ is the elevation (m), and $T$ is the mean laboratory temperature (17 °C). $P_i$ is the partial pressure of i in the atmosphere (GPa) and 760 represents the partial pressure of water vapor in air (GPa). $K_i^{gw}$ is Henrys constant for ASW generation (17 °C, 0 M and 65 m; Crovetto et al., 1982, Fernández-prini et al., 2003, Smith & Kennedy, 1983, Wagner & Pruss, 1992). All Parameters are defined in Table S1 in the supporting information.

The noble gas concentrations for each ASW analyzed were calculated using the expected concentrations for the corresponding equilibration temperature (equation (2)). Temperature differences between different ASWs generated could cause He, Ne, Ar, Kr, Xe concentration variations of 0.34%, 1.2%, 3.2%, 3.9%, and 4.9%, respectively. In order to compare all the ASW, they were all subsequently corrected to 17 °C. In addition, the signals had to be corrected for any internal machine changes (i.e., machine drift) over the 10-month period they were analyzed and normalized to the internal air standards.

$$C_i^{asw} = \frac{S_i/V_w}{S_i^{asw\ av}/V_{asw\ av}} \times C_i^{ex\ asw} \qquad (2)$$

$C_i^{asw}$ is the ASW concentration ($cm^3/cm^3$), $S_i$= corrected signal for $i$ (fA), $V_w$ is the weight of water processed ($cm^{-3}$), $V_{asw\ av}$ is the average ASW weight ($cm^{-3}$), and $S_i^{asw\ av}$ is the average ASW signal for $I$ (fA).

### 3.3. Reproducibility of Air-Saturated Waters

Concentrations for the air-derived noble gases ($^4$He, $^{20}$Ne, $^{36}$Ar, $^{84}$Kr, and $^{132}$Xe) in the water phase were calculated to be $4.5 \pm 0.1 \times 10^{-8}$ $cm^3/cm^3$, $1.7 \pm 0.1 \times 10^{-7}$ $cm^3/cm^3$, $1.1 \pm 0.1 \times 10^{-6}$ $cm^3/cm^3$, $4.4 \pm 0.2 \times 10^{-8}$ $cm^3/cm^3$, and $3.0 \pm 0.2 \times 10^{-9}$ $cm^3/cm^3$, respectively (Figure 2 and Table 2). Instrument error (associated with the internal air standards, section S2.1.) is <1.2% for all isotopes; the method reproducibility between ASWs is the most significant source of error. The elemental ratios are $^{20}$Ne/$^{36}$Ar 0.15 $\pm$ 0.01, $^{84}$Kr/$^{36}$Ar 0.039 $\pm$ 0.003, and $^{132}$Xe/$^{36}$Ar 0.0027 $\pm$ 0.0002. This is significantly less than the difference in the important natural ratios (i.e., for $^{20}$Ne/$^{36}$Ar Air = 0.52, ASW = 0.15, and an infinitely small volume of oil equilibrated with ASW = 0.04; Figure 2 and Table 2). The percentage standard error was 1.2%, 2.1%, 2.3%, 2.7%, and 2.8% for $^4$He, $^{20}$Ne, $^{40}$Ar, $^{84}$Kr, and $^{132}$Xe concentrations, respectively, in a consecutive set of five ASW noble gas determinations.

Due to the variable nature of the phases in produced water samples at the wellheads, it was not possible to collect repeatable samples to use for sample standardization. However, due to the rigorous clean-up procedure between samples, the ASWs are sufficient to determine the method reproducibility. The water salinity could be altered to match that of the samples being run if necessary.

## 4. Produced Water Results

### 4.1. Geological Context

The Fruitvale oil field is located in the south of the San Joaquin basin, within the city limits of Bakersfield, California, USA (Figure S2). Fruitvale, like most oil fields in the San Joaquin valley is characterized by spatially variable geology and hydrocarbon production depths as well as by widely varying amounts of water injection (Long et al., 2015; Division of Oil Gas and Geothermal Resources (DOGGR), 2018). Most of the water injected is produced water from oil wells, although some waste water from refineries is injected in places (Wright et al., 2019). Analyses of casing gas samples from injectate storage tanks in Fruitvale indicated substantial mixing with air (Barry, Kulongoski, et al., 2018). Geological and depositional history for the field can be found in the supporting information (Division of Oil, Gas and Geothermal Resources (DOGGR), 1992, 1998, 2017, 2018, Hluza, 1965; Lillis & Magoon, 2007; Preston, 1931, Scheirer & Magoon, 2007).

The injection and long production history have resulted in temporal variations in the total amount of hydrocarbons and produced waters being produced in the Fruitvale oil field (McMahon et al., 2018). The average reservoir temperature is 51 $^0$C and salinity is 0.095 M (Division of Oil Gas and Geothermal Resources (DOGGR), 2018). The relatively low salinity of the field compared to many oil-field waters is a result of the significant recharge over geologic timescales from the Kern River and other smaller streams draining the high altitude Sierra Nevada (McMahon et al., 2018). There has been no significant change in reservoir salinity since injection began (Stephens et al., 2018). Production data shows no evidence for gas cap formation at Fruitvale (Division of Oil Gas and Geothermal Resources (DOGGR), 1998, 2018).

### 4.2. Sample Collection

Six produced water samples were collected from the Fruitvale oil field, as part of the California State Water Resources Control Board's oil and gas regional groundwater monitoring program (RMP; Table S2). The RMP aims to determine the relations of regional water quality in aquifers located near to oil and gas sources (U.S. Geological Survey, 2019). Produced fluids in the oil wells sampled were pumped to the surface as part of
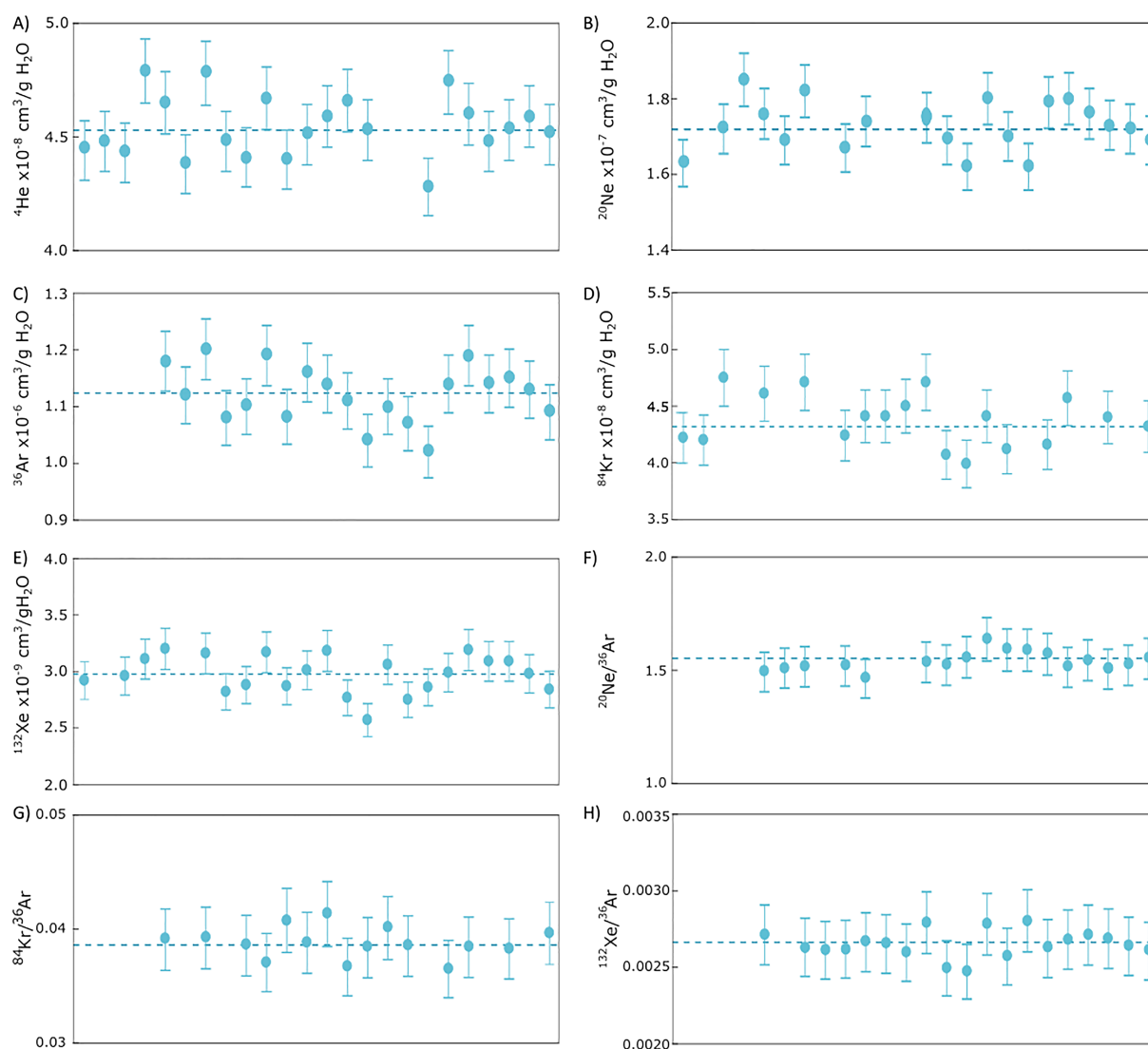
**Figure 2.** Overall reproducibility of the air-saturated water (ASW) reference materials. Mean values are given by dashed line and errors are for 1 standard deviation. (a) Reproducibility of the $^4$He concentrations across all the ASWs. Mean concentration was $4.54\pm0.13 \times 10^{-8}$ cm$^3$/cm$^3$. (b) Reproducibility of the $^{20}$Ne concentrations in the ASWs. Mean concentration was $1.73\pm0.07 \times 10^{-7}$ cm$^3$/cm$^3$. (c) Reproducibility of the $^{36}$Ar concentrations across all the ASWs. Mean concentration was $1.12\pm0.05 \times 10^{-6}$ cm$^3$/cm$^3$. (d) Reproducibility of the $^{84}$Kr concentrations in the ASWs. Mean concentration was $4.38\pm0.23 \times 10^{-8}$ cm$^3$/cm$^3$. (e) Reproducibility of the $^{132}$Xe concentrations in the ASWs run. Mean concentration was $2.98\pm0.17 \times 10^{-9}$ cm$^3$/cm$^3$. (f) Reproducibility of the elemental ratio $^{20}$Ne/$^{36}$Ar. Mean $^{20}$Ne/$^{36}$Ar was 0.15±0.009. (g) Reproducibility of the elemental ratio $^{84}$Kr/$^{36}$Ar. Mean $^{84}$Kr/$^{36}$Ar was 0.039±0.003. (h) Reproducibility of the elemental ratio $^{132}$Xe/$^{36}$Ar. Mean $^{132}$Xe/$^{36}$Ar was 0.0027±0.0002.

normal production activities and appear as surges of oil, water, and gas at a sampling port on the well discharge pipe. Measured gas-oil (GOR) and water-oil (WOR) ratios during sample collection were >2 and >41, respectively, compared to GOR= 48–76 and WOR=17–147 reported for the wells during the month of sampling (July 2016) by the Division of Oil, Gas and Geothermal Resources (Table 1; Division of Oil Gas and Geothermal Resources (DOGGR), 2018). With the exception of sample F5, where no injection has been recorded within 500 m since 1977 and is considered pristine, the samples represent wells which have been effected by the injection of produced water for EOR and waste disposal purposes.

Fluid samples were collected in 3/8" refrigeration grade copper tubes connected to sample ports at the well-head using standard noble gas sampling techniques (Burnard, 2013; Weiss, 1968). The copper tubing was flushed with produced oil well fluids prior to sampling. During water sampling, precautions are typically taken to ensure there are no bubbles present within the tubes (as noble gases preferentially partition to

**Table 2**
*Measured Concentrations in ASW (cm$^3$/cm$^3$) and Associated Ratios*

| | $^4$He | $^{20}$Ne | $^{36}$Ar | $^{84}$Kr | $^{132}$Xe | $^3$He/$^4$He (R/R$_A$) | $^{20}$Ne/$^{22}$Ne | $^{40}$Ar/$^{36}$Ar | $^{84}$Kr/$^{82}$Kr | $^{132}$Xe/$^{130}$Xe | $^{20}$Ne/$^{36}$Ar |
|---|---|---|---|---|---|---|---|---|---|---|---|
| | $\times 10^{-8}$ | $\times 10^{-7}$ | $\times 10^{-6}$ | $\times 10^{-8}$ | $\times 10^{-9}$ | | | | | | |
| Air | 520 | 170 | 31 | 65 | 24 | 1 | 9.8 | 296 | 4.9 | 6.6 | 0.52 |
| ASW at 17 °C | 4.5 | 1.7 | 1.1 | 4.3 | 2.9 | 1 | 9.8 | 296 | 4.9 | 6.6 | 0.15 |
| ASW 1 | 4.4 | 1.6 | n.d | 4.2 | 2.9 | 0.96 | 9.2 | n.d. | 4.8 | 6.5 | n.d. |
| ASW 2 | 4.5 | n.d. | n.d. | 4.2 | n.d. | 0.96 | 9.2 | n.d. | n.d. | 6.5 | n.d. |
| ASW 3 | 4.4 | 1.7 | n.d. | 4.8 | 3.0 | 1.00 | 9.5 | n.d. | 4.8 | 6.6 | n.d. |
| ASW 4 | 4.8 | 1.9 | n.d. | n.d. | 3.1 | 0.95 | 9.5 | n.d. | 4.8 | 6.6 | n.d. |
| ASW 5 | 4.7 | 1.8 | 1.2 | 4.6 | 3.2 | 1.00 | 9.6 | 301 | 4.5 | 6.6 | 0.15 |
| ASW 6 | 4.4 | 1.7 | 1.1 | n.d. | n.d. | 1.00 | 9.8 | 301 | n.d. | n.d. | 0.15 |
| ASW 7 | 4.8 | 1.8 | 1.2 | 4.7 | 3.2 | 1.00 | 9.8 | 302 | 4.5 | 6.6 | 0.15 |
| ASW 8 | 4.5 | n.d. | 1.1 | n.d. | 2.8 | 0.99 | 9.5 | 294 | 4.4 | 6.8 | n.d. |
| ASW 9 | 4.4 | 1.7 | 1.1 | 4.2 | 2.9 | n.d. | 9.6 | 300 | 4.5 | 6.5 | 0.15 |
| ASW 10 | 4.7 | 1.7 | 1.2 | 4.4 | 3.2 | 1.01 | 9.9 | 298 | 4.5 | 6.5 | 0.15 |
| ASW 11 | 4.4 | n.d. | 1.1 | 4.4 | 2.9 | 1.00 | 9.9 | 301 | 4.8 | 6.5 | n.d. |
| ASW 12 | 4.5 | n.d. | 1.2 | 4.5 | 3.0 | n.d. | 9.8 | 298 | 4.9 | 6.6 | n.d. |
| ASW 13 | 4.6 | 1.8 | 1.1 | 4.7 | 3.2 | 1.05 | 9.7 | 293 | 4.8 | 6.5 | 0.15 |
| ASW 14 | 4.7 | 1.7 | 1.1 | 4.1 | 2.8 | 0.97 | 9.7 | 292 | 4.7 | 6.4 | 0.15 |
| ASW 15 | 4.5 | 1.6 | 1.0 | 4.0 | 2.6 | 0.99 | 9.8 | 299 | 4.8 | 6.6 | 0.16 |
| ASW 16 | n.d. | 1.8 | 1.1 | 4.4 | 3.1 | n.d. | 9.7 | 291 | 4.9 | 6.4 | 0.16 |
| ASW 17 | n.d. | 1.7 | 1.1 | 4.1 | 2.8 | 1.05 | 9.3 | 292 | 4.9 | 6.4 | 0.16 |
| ASW 18 | 4.3 | 1.6 | 1.0 | n.d. | 2.9 | 1.03 | 9.3 | 292 | n.d. | 6.6 | 0.16 |
| ASW 19 | 4.7 | 1.8 | 1.1 | 4.2 | 3.0 | 1.01 | 9.5 | 295 | 4.5 | 6.6 | 0.16 |
| ASW 20 | 4.6 | 1.8 | 1.2 | 4.6 | 3.2 | 1.01 | 9.7 | 304 | 4.8 | 6.5 | 0.15 |
| ASW 21 | 4.5 | 1.8 | 1.1 | n.d. | 3.1 | 1.01 | 9.7 | 303 | n.d. | 6.5 | 0.15 |
| ASW 22 | 4.5 | 1.7 | 1.2 | 4.4 | 3.1 | 1.00 | 9.6 | 304 | 4.5 | 6.5 | 0.15 |
| ASW 23 | 4.6 | 1.7 | 1.1 | n.d. | 3.0 | 0.98 | 9.7 | 304 | n.d. | 6.5 | 0.15 |
| ASW 24 | 4.5 | 1.7 | 1.1 | 4.3 | 2.8 | 1.00 | 9.7 | 305 | 4.8 | 6.5 | 0.15 |
| Average ASW | 4.5 | 1.7 | 1.1 | 4.4 | 3.0 | 1.00 | 9.6 | 299 | 4.7 | 6.5 | 0.15 |
| Standard error (%) | 2.9 | 3.8 | 4.5 | 5.3 | 5.7 | 2.7 | 2.0 | 1.6 | 3.6 | 1.2 | 5.9 |

*Note.* Errors are given for 1 standard deviation.
Abbreviation: n.d.: not determined.

the gas phase); however, as produced fluids are variable mixtures of water, oil, and gas in variable quantities, gas was inherently present within these oil well samples. Copper tubes were connected to the wellhead sampling port using reinforced polytetrafluoroethylene tubing and hose clamps were used to seal each sample from atmospheric exposure. A "T" was fitted at the wellhead to ensure the tubing did not become over-pressurized once the copper tubes were sealed with stainless steel clamps. Complementary casing gases were not available for collection from oil wells sampled at Fruitvale; this made it an ideal location to test what could be learnt solely from produced water samples.

### 4.3. Calculating Concentrations in Multiphase Samples

Total concentration of noble gases within the sampled Cu tube can be calculated using equation (2), where $C_i^{\text{asw}}$ is replaced with the total concentration in the sample $C_i^S$ (cm$^3$/cm$^3$) and $V_w$ is replaced with the total volume of the Cu tube sampled ($V_t$[cm$^3$]). The total number of mols of noble gases ($n_i^t$ [mol]) within the sample can be calculated using equation (3). The total amount of the noble gases within in the Cu tube will not change between production and analysis.

$$n_i^t = \frac{C_i^s \times V_t}{22413} \tag{3}$$

Produced fluid samples contain variable mixtures of water, gas, and oil; therefore, it is important to consider the concentration of noble gas in each phase. To calculate the concentration of noble gas in each phase at the time of sampling, the relative solubilities (Henry's constants) of the noble gases within each phase in the Cu tube must be calculated under production temperature, sample salinity and oil density. For the gas water

equilibrium, the solubility coefficient ($K_i^{gw}$, atm kg/mol) can be calculated in the same way as for ASW (Crovetto et al., 1982; Fernández-prini et al., 2003; Smith & Kennedy, 1983; Wagner & Pruss, 1992). The solubility coefficients between a gas and oil phase ($K_i^{go}$, atm kg/mol) are calculated using Kharaka and Specht (1987) and Smith and Kennedy (1983). The expected distribution of noble gases between the phases within the Cu tube can then be calculated. The amount in the oil, gas, and water phase is calculated relative to each other using equations (4) and (5).

$$n_i^o = \frac{n_i^g \times V_o}{K_i^{go} \times V_g} \tag{4}$$

$$n_i^w = \frac{n_i^g \times V_w}{K_i^{gw} \times V_g} \tag{5}$$

where $n_i^g$ is the amount in the gas phase. As just the relative proportions of water, oil, and gas are required, any value can be used for $n_i^g$. The concentration of the noble gases between the phases can then be calculated using equations (6)–(8).

$$C_i^g = \frac{n_i^t \times n_i^g}{(n_i^g + n_i^o + n_i^w) \times V_g} \tag{6}$$

$$C_i^o = \frac{n_i^t \times n_i^o}{(n_i^g + n_i^o + n_i^w) \times V_o} \tag{7}$$

$$C_i^w = \frac{n_i^t \times n_i^w}{(n_i^g + n_i^o + n_i^w) \times V_w} \tag{8}$$

where $C_i^g$, $C_i^o$, and $C_i^w$ are the concentration in the gas, oil and water phase, respectively, in mol/cm$^3$. All parameters are defined in Table S1.

The variable nature of the produced water compositions at the wellhead means that the WOR and GOR are not consistent during sampling and are not representative of the average GOR and WOR for production (Table 1). As a result, a collected sample may not contain all three phases. By assuming that the phases are in equilibrium at the wellhead, the concentration in the missing phase can be calculated using equations (9) and (10).

$$K_i^{go} = \frac{C_i^g}{C_i^o} \tag{9}$$

$$K_i^{gw} = \frac{C_i^g}{C_i^w} \tag{10}$$

The concentration of noble gases between the three phases at the point of production can be found in Table S3. The concentrations in the Cu tube were originally reported in Gannon et al. (2018) in cm$^3$/g (total fluid) at standard temperature and pressure; these values can be converted to the total amount of noble gases in the Cu tube ($n_i^t$) by multiplying by ($V_w + V_o$). It is important to note that it is assumed that solubility equilibrium has been reached at the wellhead between all phases. If equilibrium has not been reached, the results will be skewed.

### 4.4. Produced Water Compositions

Concentrations of noble gases in both the oil and water phases are significantly depleted in comparison to the gas phase and ASW for recharge conditions at the Fruitvale oil field (15 °C, 0 M, 123 m; Table S3). The gas phase is likely to resemble the composition expected within casing gas samples. The oil and water phase have similar concentrations for the lighter noble gases; however, there is a noticeable enrichment of Kr and Xe within the oil phases due to their higher solubility in oil. Within each phase, concentrations range by up to two orders of magnitude. $^{20}$Ne concentrations range from $0.42 \pm 0.02$ to $57 \pm 3 \times 10^{-12}$ mol/cm$^3$ in the gas phase, $0.22 \pm 0.01$ to $35 \pm 2 \times 10^{-15}$ mol/cm$^3$ in the oil phase and $0.19 \pm 0.01$ to $25 \pm 1 \times 10^{-15}$ mol/cm$^3$ in the water phase (Table S3). Single-element isotope ratios are consistent throughout all the samples; however, the elemental ratios show significant difference between the samples and phases. For example

the $^{20}Ne/^{36}Ar$ in the gas phase ranges from 0.080 ± 0.005 to 0.40 ± 0.03, from 0.0065 ± 0.0005 to 0.033 ± 0.002 in the oil phase, and 0.029 ± 0.002 to 0.15 ± 0.01 in the water phase.

Blank contributions to the samples analyzed were <0.40% He, <1.5% Ne, <1.5% Ar, <0.15% Kr, and <0.020% Xe, suggesting that the main source of analytical uncertainty on the concentrations is from the variability in the ASW reproducibility.

## 5. Conclusions

A newly designed noble gas extraction system, interfaced with a gas purification system, automated preparatory system and Argus IV and Helix SFT mass spectrometers, has been constructed to allow multi-phase oil-water-gas samples from oil wells to be separated and the fluids analyzed for their noble gas abundance and isotopic composition. We are able to reproducibly purify and measure noble gases from air-saturated waters and produced fluids using this system. The reproducibility of the ASW reference material was within 2.9% for $^4He$, 3.8% for $^{20}Ne$, 4.5% for $^{36}Ar$, 5.3% for $^{84}Kr$, and 5.7% for $^{132}Xe$. We demonstrate the need for and advantages of this new system, which allows us to fully characterize oil field fluids without damaging the ultra-high vacuum systems required for noble gas analysis.

The system was tested for concentrations and isotope ratios with six produced fluid samples from oil wells in the Fruitvale oil field, California. The oil and water phases are significantly depleted in noble gases compared to the gas phase and ASW. The ability to calculate noble gas concentrations in each of the phases means produced fluids alone can be effective samples for geochemically characterizing hydrocarbon systems and could be used in similar ways to casing gases to reconstruct hydrocarbon reservoir compositions. Once the reservoir has been fully characterized, reservoir evolution can be modeled, which will be critical when identifying if there is a presence of fugitive gases in overlying aquifers, and if present, determining their source.

## References

Ballentine, C. J., Burgess, R., & Marty, B. (2002). Tracing Fluid Origin, Transport and Interaction in the Crust. In D. Porcelli, C. J. Ballentine, & R. Wieler (Eds.), *Noble Gases in Geochemistry and Cosmochemistry*, (pp. 539–614). America, Chap.13: Geochemical Society, Mineralogical Society of America.

Ballentine, C. J., O'Nions, R. K., & Coleman, M. L. (1996). A Magnus opus: Helium, neon, and argon isotopes in a North Sea oilfield. *Geochimica et Cosmochimica Acta*, *60*(5), 831–849. https://doi.org/10.1016/0016-7037(95)00439-4

Ballentine, C. J., O'Nions, R. K., Oxburgh, E. R., Horvath, F., & Deak, J. (1991). Rare gas constraints on hydrocarbon accumulation, crustal degassing and groundwater flow in the Pannonian Basin. *Earth and Planetary Science Letters*, *105*(1-3), 229–246. https://doi.org/10.1016/0012-821X(91)90133-3

Barry, P. H., Kulongoski, J. T., Landon, M. K., Tyne, R. L., Gillespie, J., Stephens, M., et al. (2018). Tracing enhanced oil recovery signatures in casing gases using noble gases. *Earth and Planetary Science Letters*, *496*, 57–67. https://doi.org/10.1016/j.epsl.2018.05.028

Barry, P. H., Lawson, M., Meurer, W. P., Cheng, A., & Ballentine, C. J. (2018). Noble gases in deep-water oils of the U.S. Gulf of Mexico. *Geochemistry, Geophysics, Geosystems*, *19*, 4218–4235. https://doi.org/10.1029/2018GC007654

Barry, P. H., Lawson, M., Meurer, W. P., Danabalan, D., Byrne, D. J., Mabry, J. C., & Ballentine, C. J. (2017). Determining fluid migration and isolation times in multiphase crustal domains using noble gases. *Geology*, *45*(9), 775–778. https://doi.org/10.1130/G38900.1

Barry, P. H., Lawson, M., Meurer, W. P., Warr, O., Mabry, J. C., Byrne, D. J., & Ballentine, C. J. (2016). Noble gas solubility models of hydrocarbon charge mechanism in the Sleipner Vest gas field. *Geochimica et Cosmochimica Acta*, *194*, 291–309. https://doi.org/10.1016/j.gca.2016.08.021

Bayerle, U., Aeschbach-Hertig, W., Imboden, D. M., Baur, H., Graf, T., & Kipfer, R. (2000). A mass spectrometric system for the analysis of noble gases and tritium from water samples. *Environmental Science & Technology*, *34*(10), 2042–2050. https://doi.org/10.1021/es990840h

Bosch, A., & Mazor, E. (1988). Natural gas association with water and oil as depicted by atmospheric noble gases: Case studies from the southeastern Mediterranean Coastal Plain. *Earth and Planetary Science Letters*, *87*(3), 338–346. https://doi.org/10.1016/0012-821X(88)90021-0

Burnard, P. (2013). *The Noble Gases as Geochemical Tracers*. Berlin, Heidelberg: Springer.

Byrne, D. J., Barry, P. H., Lawson, M., & Ballentine, C. J. (2018a). Noble gases in conventional and unconventional petroleum systems. *Geological Society of London, Special Publication*, *468*(1), 127–149. https://doi.org/10.1144/SP468.5

Byrne, D. J., Barry, P. H., Lawson, M., & Ballentine, C. J. (2018b). Determining gas expulsion vs retention during hydrocarbon generation in the Eagle Ford Shale using noble gases. *Geochimica et Cosmochimica Acta*, *241*, 240–254. https://doi.org/10.1016/j.gca.2018.08.042

Crovetto, R., Fernández-Prini, R., & Japas, M. L. (1982). Solubilities of inert gases and methane in $H_2O$ and in $D_2O$ in the temperature range of 300 to 600 K. *The Journal of Chemical Physics*, *76*(2), 1077–1086. https://doi.org/10.1063/1.443074

Darrah, T. H., Jackson, R. B., Vengosh, A., Warner, N. R., Whyte, C. J., Walsh, T. B., et al. (2015). The evolution of Devonian hydrocarbon gases in shallow aquifers of the northern Appalachian Basin: Insights from integrating noble gas and hydrocarbon geochemistry. *Geochimica et Cosmochimica Acta*, *170*, 321–355. https://doi.org/10.1016/j.gca.2015.09.006

Darrah, T. H., Vengosh, A., Jackson, R. B., Warner, N. R., & Poreda, R. J. (2014). Noble gases identify the mechanisms of fugitive gas contamination in drinking-water wells overlying the Marcellus and Barnett Shales. *Proceedings of the National Academy of Sciences*, *111*(39), 14,076–14,081. https://doi.org/10.1073/pnas.1322107111

Division of Oil Gas and Geothermal Resources (DOGGR) (1998). *California Oil and Gas Fields: Volume 1- Central California.TR11*. Sacramento, CA: California Department of Conservation.

Division of Oil Gas and Geothermal Resources (DOGGR) (2017). GIS Mapping, DOGGR, Sacramento, CA. http://www.conservation.ca.gov/dog/maps/Pages/GISMapping2.aspx (Accessed online May 2017).

Division of Oil Gas and Geothermal Resources (DOGGR) (2018). Oil & Gas Online Data. Division of Oil, Gas, and Geothermal Resources. http://www.conservation.ca.gov/dog/Online_Data/Pages/Index.aspx (accessed October 23, 2018).

Division of Oil, Gas and Geothermal Resources (DOGGR) (1992). California Oil and Gas Fields Volume II - Southern, Central Coastal, and Offshore California Oil and Gas Fields. California Department of Conservation, Sacramento, CA.

Fernández-prini, R., Alvarez, J. L., Harvey, A. H., & Ferna, R. (2003). Henry's Constants and Vapor – Liquid Distribution Constants for Gaseous Solutes in $H_2O$ and $D_2O$ at High Temperatures Henry's Constants and Vapor. *Journal of Physical and Chemical Reference Data*, *32*(2), 903–916. https://doi.org/10.1063/1.1564818

Gannon, R.S., Saraceno, J.F., Kulongoski, J.T., Teunis, J.A., Barry, P.H., Tyne, R.L., et al., 2018. Produced Water Chemistry Data for the Lost Hills, Fruitvale, and North and South Belridge Study Areas, Southern San Joaquin Valley, California. 2016–17: U.S. Geological Survey Data Release.

Gilfillan, S. M. V., Ballentine, C. J., Holland, G., Blagburn, D., Lollar, B. S., Stevens, S., et al. (2008). The noble gas geochemsitry of natural CO2 gas reservoirs from the Colorado Plateau and Rocky Mountain provinces, USA. *Geochimica et Cosmochimica Acta*, *72*(4), 1174–1198. https://doi.org/10.1016/j.gca.2007.10.009

Gilfillan, S. M. V., Haszeldine, R. S., Stuart, F. M., Gyore, D., Kilgallon, R., & Wilkinson, M. (2014). The application of noble gases and carbon stbale isotopes in tracing the fate, migration and storage of $CO_2$. *Energy Procedia*, *63*, 4123–4133. https://doi.org/10.1016/j.egypro.2014.11.443

Gilfillan, S. M. V., Sherk, G. W., Poreda, R. J., & Haszeldine, R. S. (2017). Using noble gas fingerprints at the Kerr Farm to assess $CO_2$ leakage allegations linked to the Weyburn-Midale $CO_2$ monitoring and storage project. *International Journal of Greenhouse Gas Control*, *63*, 215–225. https://doi.org/10.1016/j.ijggc.2017.05.015

Györe, D., Gilfillan, S. M. V., & Stuart, F. M. (2017). Tracking the interaction between injected $CO_2$ and reservoir fluids using noble gas isotopes in an analogue of large scale carbon cpature and storage. *Applied Geochemistry*, *78*, 116–128. https://doi.org/10.1016/j.apgeochem.2016.12.012

Györe, D., Stuart, F. M., Gilfillan, S. M. V., & Waldron, S. (2015). Tracing injected $CO_2$ in the cranfield enhance oil recovery field (MS, USA) using He, Ne and Ar isotopes. *International Journal of Greenhouse Gas Control*, *42*, 554–561. https://doi.org/10.1016/j.ijggc.2015.09.009

Harkness, J. S., Darrah, T. H., Warner, N. R., Whyte, C. J., Moore, M. T., Millot, R., et al. (2017). The geochemistry of naturally occurring methane and saline groundwater in an area of unconventional shale gas development. *Geochimica et Cosmochimica Acta*, *208*, 302–334. https://doi.org/10.1016/j.gca.2017.03.039

Hillegonds, D J., Matsumoto, T., Manfred, J., Han, LF., Klaus, P, Wassenaar, L., Pradeep, A., 2013. Calibration of Dissolved Noble Gas Mass Spectrometric Measurements by an Air-Water Equilibration System. EGU General Assembly 2013, 7-12 April, Vienna, Austria.

Hluza, A. G. (1965). *Summary of operations, California oil fields*, (Vol. 51). California: Department of Conservation, Sacramento, Ca.

Holland, G., & Gilfillan, S. M. V. (2013). Application of noble gases to the viability of CO2 storage. In P. Burnard (Ed.), *The Noble Gases as Geochemical Tracers*, (pp. 177–223). Berlin, Heidelberg: Springer.

Hunt, A.G., (2015). Noble Gas Laboratory's standard operating procedures for the measurement of dissolved gas in water samples: U.S. Geological Survey Techniques and Methods 5- A11. U.S. Geological Survey, Reston, Virginia

Kharaka, Y. K., & Specht, D. J. (1988). The solubility of noble gases in crude oil at 25-100 $^0$C. *Applied Geochemistry*, *3*(2), 137–144. https://doi.org/10.1016/0883-2927(88)90001-7

Lillis, P. G., Magoon, L. B. (2007). Petroleum Systems of the San Joaquin Basin Province—Geochemical Characteristics of Oil Types. In A.H. Scheirer eds. Petroleum Systems and Geological Assessment of oil and gas in the san Joaquin Basin Province, California. USGS professional paper, Sacramento, Ca. Chapter 9 1-52. https://doi.org/10.3133/pp17139

Long, J. C. S., Feinstein, L. C., Dirkholzer, J., Jordan, P., Houseworth, J., Dobson, P. E., et al. (2015). Historical and current application of well stimulation technology in California. In *An Independent Scientific Assessment of Well Stimulation in California*, (Vol. *1*, pp. 1-371 ). Sacramento, Ca. Chap: California Council on Science and Technology.

McMahon, P. B., Kulongoski, J. T., Vengosh, A., Cozzarelli, I. M., Landon, M. K., Kharaka, Y. K., et al. (2018). Regional Patterns in the geochemistry of oil-field water, southern San Joaquin Valley, California, USA. *Applied Geochemistry*, *98*, 127–140. https://doi.org/10.1016/j.apgeochem.2018.09.015

Pinti, D. L., & Marty, B. (1995). Noble gases in crude oils from the Paris Basin, France: Implications for the origin of fluids and constraints on oil-water-gas interactions. *Geochimica et Cosmochimica Acta*, *59*(16), 3389–3404. https://doi.org/10.1016/0016-7037(95)00213-J

Preston, H. M. (1931). Summary of operations, Calinforia oil field, Vol 16. California Department of naturla resources. Division of oil and gas.

Prinzhofer, A. (2013). Noble gases in oil and gas accumulations. In *The Noble Gases as Geochemical Tracers*, (pp. 225–247). Berlin, Heidelberg: Springer.

SAES Getters, 1986. Operating Instructions for SORB-AC cartridge pumps. SAES Getters Group manufacturing company. Milan, Italy.

Scheirer, A. H., & Magoon, L. B. (2007). Age, distribution, and stratigraphic relationship of rock units in the San Joaquin Basin Province, California. In A. H. Scheirer (Ed.), *Petroleum Systems and Geologic Assessment of Oil and Gas in the San Joaquin Basin Province, California. U.S. Geol. Surv. Prof. Paper 1713, (Ch 5, 1-107)*. Reston, Virginia: U.S. Geological Survey. https://doi.org/10.3133/pp17135

Smith, S. P., & Kennedy, B. M. (1983). The solubility of noble gases in water and in NaCl brine. *Geochimica et Cosmochimica Acta*, *47*(3), 503–515. https://doi.org/10.1016/0016-7037(83)90273-9

Stephens, M. J., Shimabukuro, D. H., Gillespie, J. M., & Chang, W. (2018). Groundwater salinity mapping using geophysical log analysis within the Fruitvale and Rosedale Ranch oil fields: Kern County, California, USA. *Hydrogeology Journal*, *27*(2), 731–746.

Stout, V. L., & Gibbons, M. D. (1955). Gettering of gas by titanium. *Journal of Applied Physiology*, *26*(12), 1488–1492. https://doi.org/10.1063/1.1721936

U.S. Geological Survey, 2019, California Oil, Gas, and Groundwater (COGG) Progra.: at: https://ca.water.usgs.gov/projects/oil-gas-groundwater/index.html (accessed February, 2019).

Vengosh, A., Jackson, R. B., Warner, N., Darrah, T. H., & Kondash, A. (2014). A Critical Review of the Risks to Water Resources from Shale Gas Development and Hydraulic Fracturing in the United States. *Environmental Science & Technology*, *16*, 6838.

Wagner, W., & Pruss, A. (1992). International Equations for the Saturation Properties of Ordinary Water Substance . Revised According to the International Temperature Scale of 1990. Addendum to J. International Equations for the Saturation Properties of Ordinary Water Substance. *Journal of Physical and Chemical Reference Data*, *893*, 1–6.

Weiss, R. F. (1968). Piggyback sampler for dissolved gas studies on sealed water samples. *Deep Sea Research and Oceanographic Abstracts*, *15*(6), 695–699. https://doi.org/10.1016/0011-7471(68)90082-X

Wright, M.T., McMahon, P.B., Landon, M.K., LAKulongoski, J.T. (2019). Groundwater quality of a public supply aquifer in promixity to oil development, Fruitvale Oil Filed, Bakersfield, California. Applied Geochemistry, *106*, 82–95. https://doi.org/10.1016/j.apgeochem.2019.05.003

Zhou, Z., Ballentine, C.J., Kipfer, R., Schoell, M., Thibodeaux, S., 2005. Noble gas tracing of groundwater/coalbed methane interaction in the San Juan Basin, USA. Geochimica et Cosmochimica Acta, 69(23), 5413-5428. https://doi.org/10.1016/j.gca.2005.06.027